Electronic Supplementary Material (ESI) for RSC Advances.

Self-assembly of Upconversion Nanoclusters with Amphiphilic Copolymer for Near-Infrared- and Temperature- Triggered Drug Release

Kai Yan, Min Chen, Shuxue Zhou and Limin Wu[1]

Department of Materials Science and State Key Laboratory of Molecular Engineering of Polymers, Fudan University, Shanghai 200433, China

Synthesis of SPIO

Monodisperse SPIO were prepared by chemical co-precipitation, followed by modification with oleic acid as follows: 13.05 g $FeCl_3 \cdot 6H_2O$ and 6.5 g $FeCl_2 \cdot 6H_2O$ were added in 80 mL water in a 250 mL four-neck flask, and degassed by the bubble of nitrogen for 30 min, and then added dropwise by 45 mL $NH_3 \cdot H_2O$ till pH=10 in order to produce black iron oxide precipitates. After the solution was heated to 75 ^oC for 1 h and 4 g of oleic acid was added, the reaction was carried out for another 1.5 h. The black nanocrystals were cooled and washed by ethanol and hexane. The final ferrofluid was dispersed in hexane for further use.

[1] Corresponding author, email: lmw@fudan.edu.cn

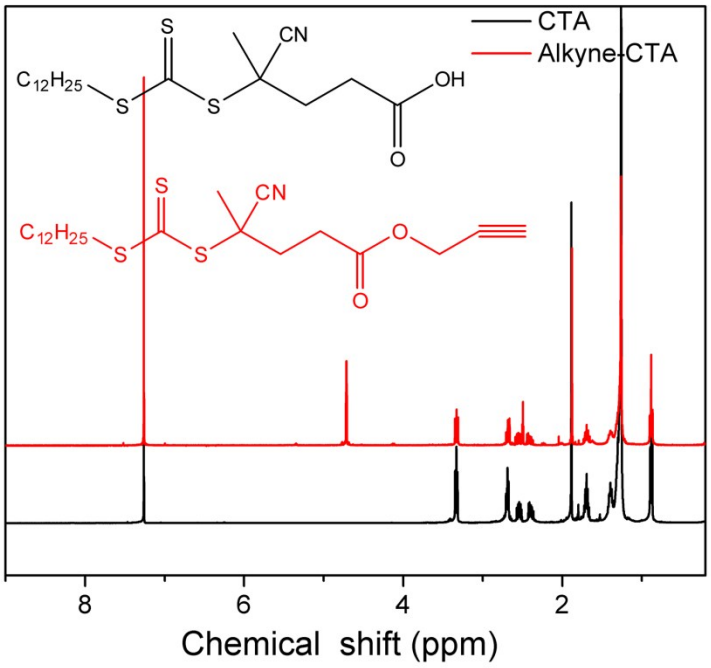

Figure S1. The structures of CTA and Alkyne-CTA were confirmed by ^{1}H NMR (500 MHz, $CDCl_3$, TMS) δ [ppm]. **CTA:**0.88 (t, 3H, $CH_3CH_2CH_2$), 1.22-1.49 (br s, 18H, $(CH_2)_9$), 1.69 (m, 2H, CH_2CH_2S), 1.88 (s, 3H, CH_3), 2.39–2.67 (m, 4H, CH_2CH_2–COO), 3.33(t, 3H, CH_2CH_2S); **Alkyne-CTA:** 0.88 (t, 3H, $CH_3CH_2CH_2$), 1.22-1.49 (br s, 18H, $(CH_2)_9$), 1.69 (m, 2H, CH_2CH_2S), 1.88 (s, 3H, CH_3), 2.39–2.67 (m, 4H, CH_2CH_2–COO), 2.49 (t, H, $OCH_2C{\equiv}CH$), 3.31, (t, 3H, CH_2CH_2S), 4.71 (d, 2H, $OCH_2C{\equiv}CH$).

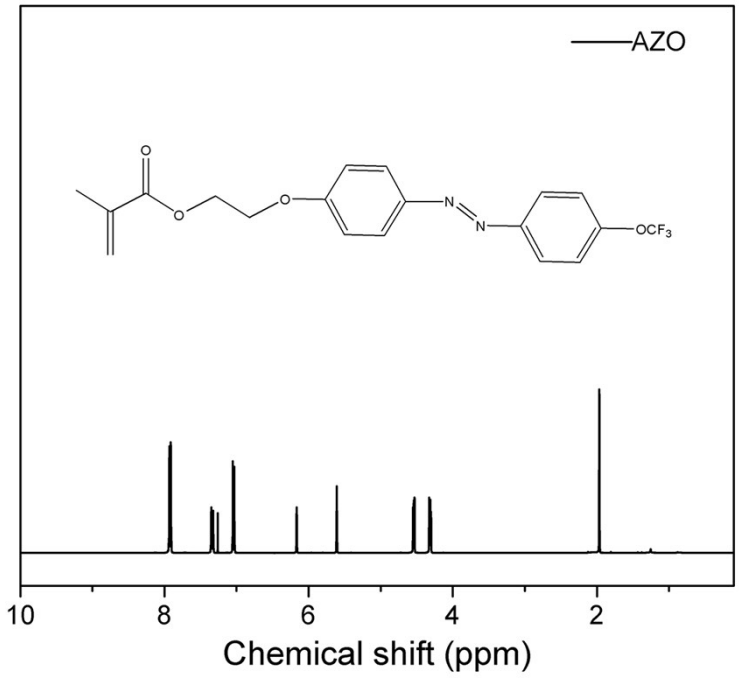

Figure S2. The structure of AZO was confirmed by ^{1}H NMR (500 MHz, $CDCl_3$, TMS) δ [ppm]: 1.97 (3H, s, CH), 4.32 (2H, t, CH_2O), 4.54 (2H, t, CH_2O), 5.61 (1H, s, CH_2=), 6.18 (1H, s, CH_2=), 7.05 (2H, d, Ar-H), 7.35 (2H, d, Ar-H), 7.93 (4H, t, Ar-H).

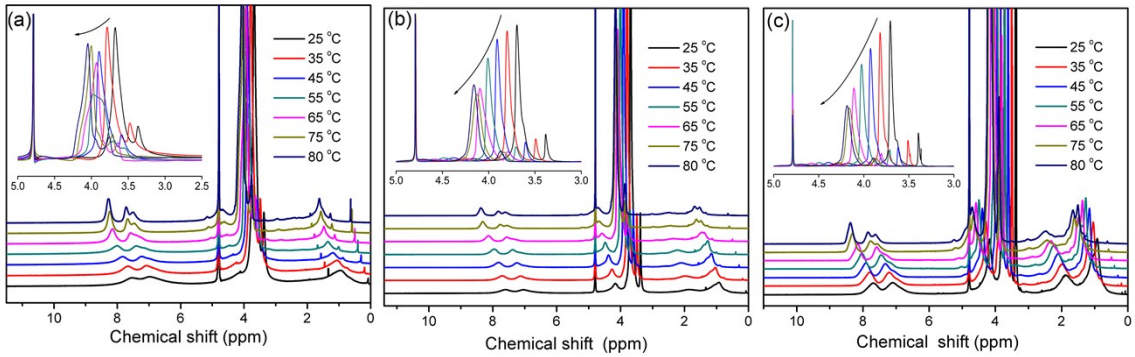

Figure S3. The corresponding ^{1}H NMR spectra at different temperature from 25 °C to 80°C.(a)poly(AZO_7-co-$OEGMA_9$),(b)poly(AZO_7-co-$OEGMA_{18}$),(c)poly(AZO_7-co-$OEGMA_{27}$).

The ^{1}H NMR spectra of these copolymer micelles in D_2O at different temperature shown in **Figure 3**a-c further confirms the temperature responsive property. As the temperature increases, the azobenzene signals (7-8 ppm) of poly(AZO-co-OEGMA)

transfer towards the higher chemical shifts. In particular, when the temperature approaches 75 ^{o}C, the proton peaks (7.6 ppm) of azobenzene are expelled and divided into two peaks, indicating the change in the average conformations of azobenzene group. Also, the OEGMA signals (3.93 ppm) of poly(AZO_7-co-$OEGMA_9$) copolymer are slightly broadened at the 55 ^{o}C due to the collapse of the polymer micelles. In contrast, the OEGMA signals of the poly(AZO_7-co-$OEGMA_{18}$) and poly(AZO_7-co-$OEGMA_{27}$) copolymers are becoming smaller and smaller, and finally stable at 70 ^{o}C and 75 ^{o}C (see the insets in Figure S3, respectively. All these results further confirm that the LCST of copolymers increases significantly with the increasing content of OEGMA.

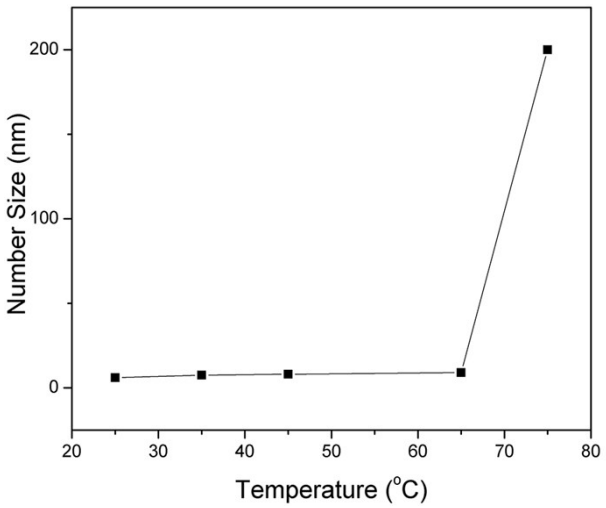

Figure S4. Number average size distributions of poly(AZO_7-co-$OEGMA_{18}$) determined by DLS at variable temperatures after UV irradiation.

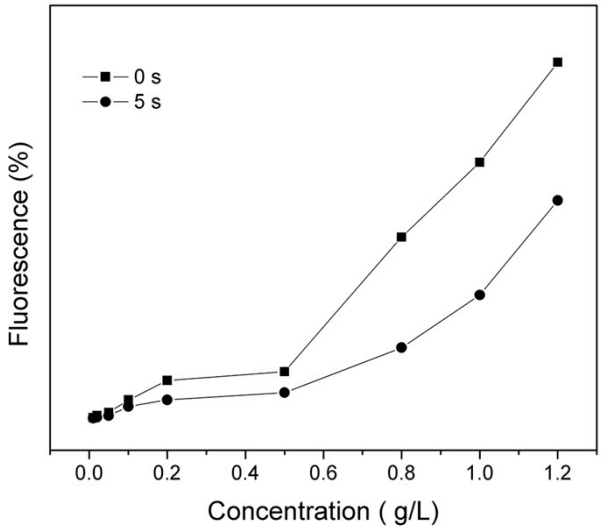

Figure S5. Fluorescence intensity of poly(AZO_7-$OEGMA_9$) before and under UV irradiation for 5s at different concentration

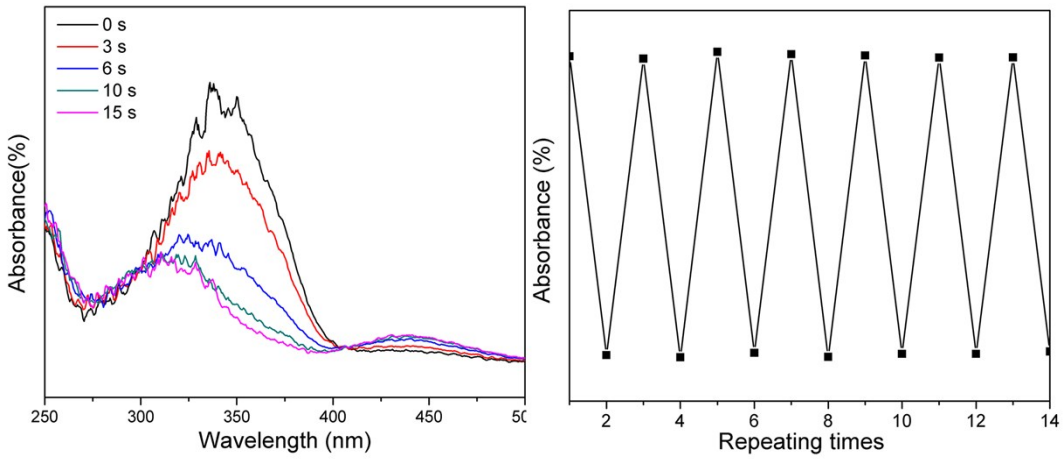

Figure S6. Photochemical processes of poly(AZO_7-$OEGMA_9$) under UV irradiation of 365 nm light for different times (left), and different recycle under UV/Vis irradiation.

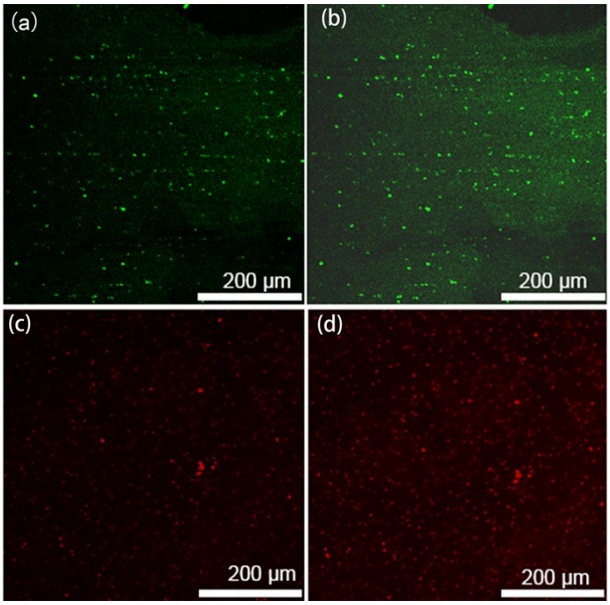

Figure S7. CLSM images (a) FITC- and (c) RhB-loaded poly(AZO_7-$OEGMA_9$) before, and after UV irradiation for 1 min of the (b) FITC- and (d) RhB-loaded poly(AZO_7-$OEGMA_9$)

The CLSM images (Figure S7a and c) can visualize the FITC- and RhB-loaded assembled structures resembling green and red spherical micelles, indicating successful encapsulation of various dyes. The CLSM image in Figure S7b and d further provided a visual sense to monitor release of FITC and RhB to exterior solution after UV irradiation, suggesting that the micelles can be used for loading and controlled release of guests through UV/Vis response.

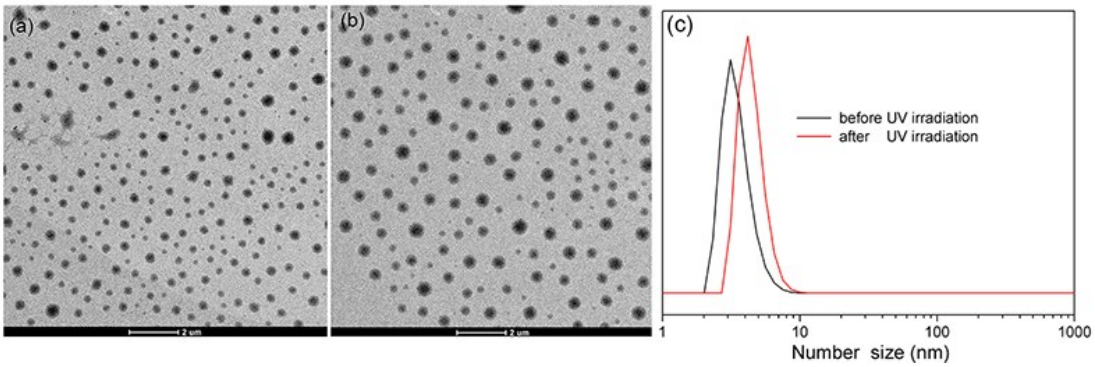

Figure S8. TEM images (a) and (b) of the micelles from poly(AZO_7-co-$OEGMA_9$) before and after UV irradiation for 20s, the changes of number size before and after UV irradiation for 20s (c)

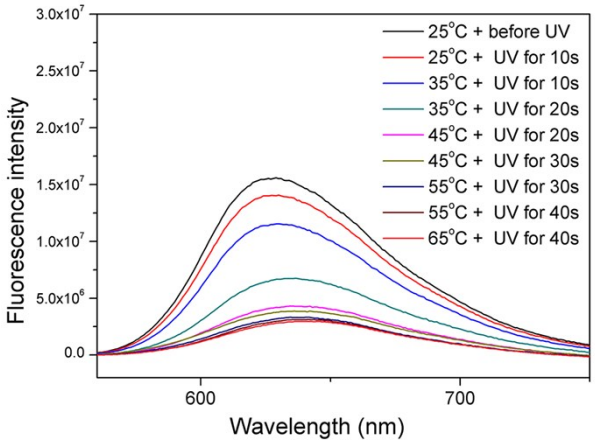

Figure S9. Fluorescence spectra of poly(AZO_7-co-$OEGMA_9$) copolymer (2.2 mg /ml) solution encapsulated with Nile Red under the irradiations of UV light and different temperature

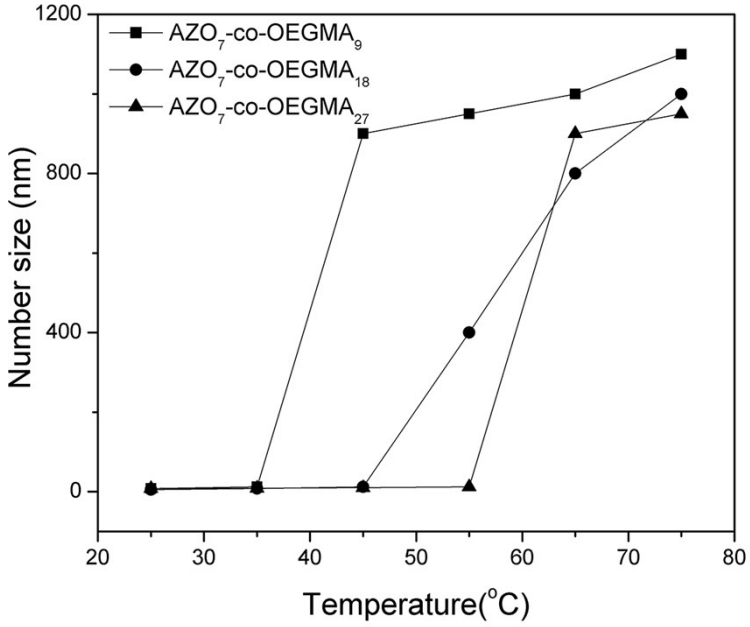

Figure S10. Changes of DLS size of poly(AZO-co-OEGMA) with various molecular weights in 0.1 M K_2SO_4 solution at variable temperatures.

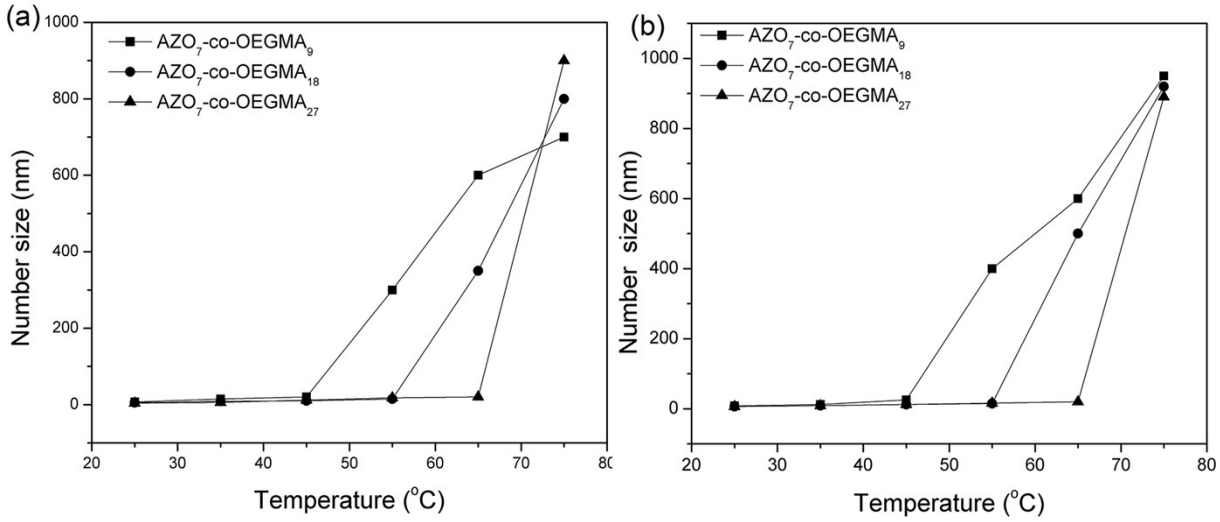

Figure S11. Changes of DLS size of poly(AZO-co-OEGMA) with various molecular weights at variable temperatures in 0.1M NaCl solution(a), 0.1M KCl solution(b).

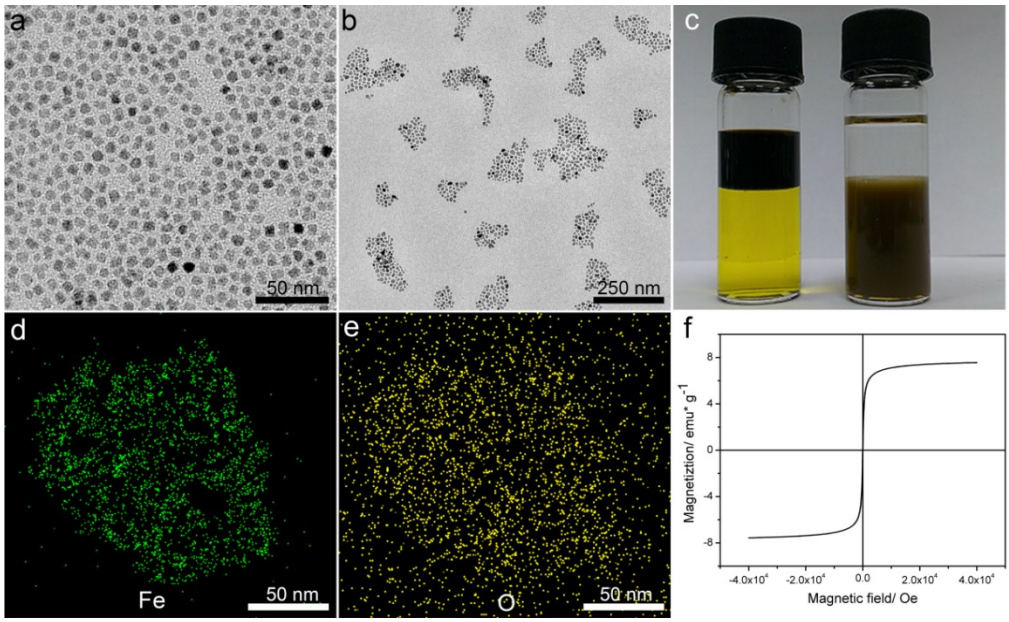

Figure S12. HRTEM images of SPIO in hexane (a) and SPIO nanoclusters in aqueous phase (b), photographs of SPIO in hexane (c, left) and SPIO nanoclusters in aqueous phase (c, right), elemental (Fe, O) mappings of the SPIO nanoclusters (d-e), (f) magnetic hysteresis loops of SPIO nanoclusters.

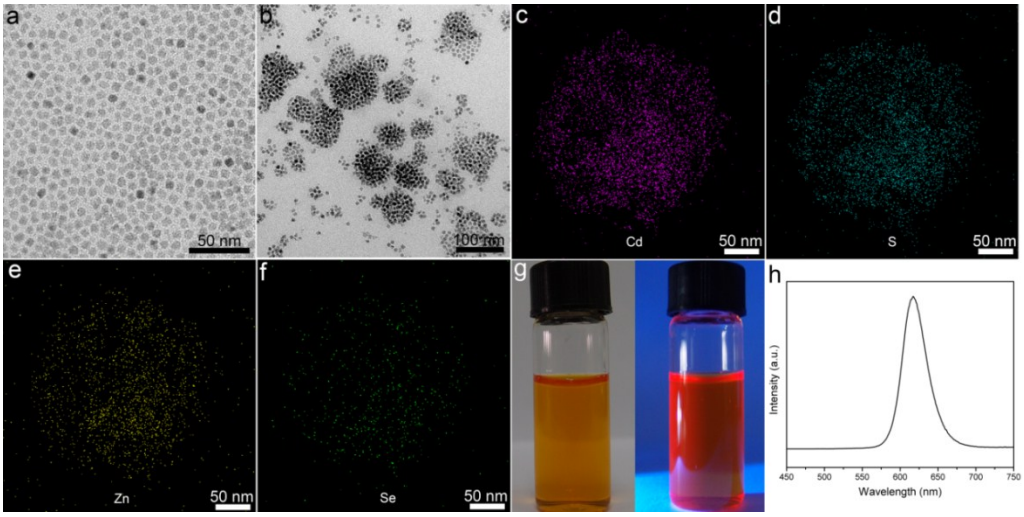

Figure S13. HRTEM images of CdSe/ZnS core-shell QD in hexane (a), QD nanoclusters in aqueous phase (b). Elemental (Cd, S, Zn, and Se) mappings of the QD nanoclusters (c-f). Photographs of QD nanoclusters in aqueous phase under daylight (g, left) and UV light (g, right). (h) Fluorescence spectra of QD nanoclusters in aqueous phase by excitation at 420 nm.

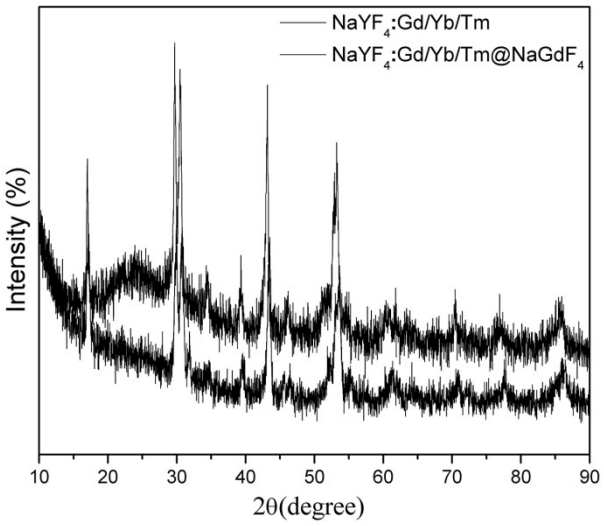

Figure S14. Powder X-ray diffraction pattern of the $NaYF_4$:Gd/Yb/Tm and $NaYF_4$:Gd/Yb/Tm@ $NaGdF_4$ nanocrystals

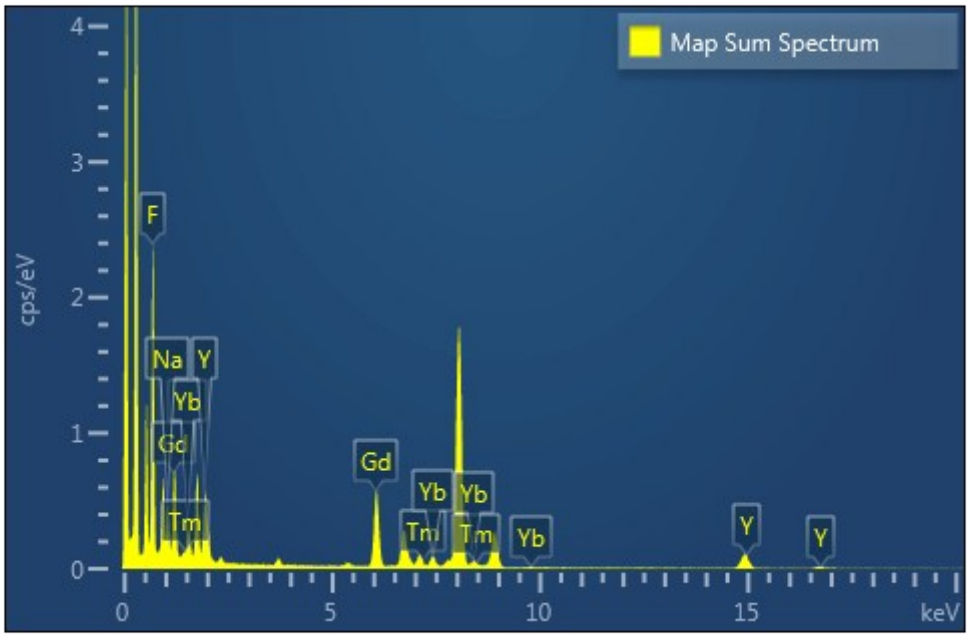

Figure S15 EDX spectrum of the $NaYF_4$:Gd/Yb/Tm@ $NaGdF_4$